Boundary Proximity Effect of an E-field Probe for SAR Measurement

Youn-Myoung Gimm, Young-Jun Ju
Graduate School of Dankook University
San 8, Hannam-dong, Yongsan-gu, Seoul 140-714, Korea
gimm@dku.edu

1. Introduction

Exposure to electromagnetic fields at frequencies above about 100 kHz can lead to significant absorption of energy and temperature increases. In general, exposure to a uniform (plane-wave) electromagnetic field results in a highly non-uniform deposition and distribution of energy within the body, which must be assessed by dosimetric measurement and calculation [1].

One means to evaluate compliance with specific SAR requirements is by measurement of the electric field strength in tissue-equivalent medium using anthropomorphic models of the human head.

$$SAR = \sigma |E|^2 / \rho \qquad (1)$$

where σ is the electrical conductivity, |E| is the rms magnitude of the electric field strength vector, and ρ is the mass density of the medium. For the purposes of the dosimetry, the head tissue density is assumed to be 1000 kg/m^3, with corresponding 1 g and 10 g averaging volumes of 1 cm^3 and 10 cm^3, respectively.

Each sensor of the probe in Fig 1 (right) for measuring SAR consists of the components in Fig 1 (left).

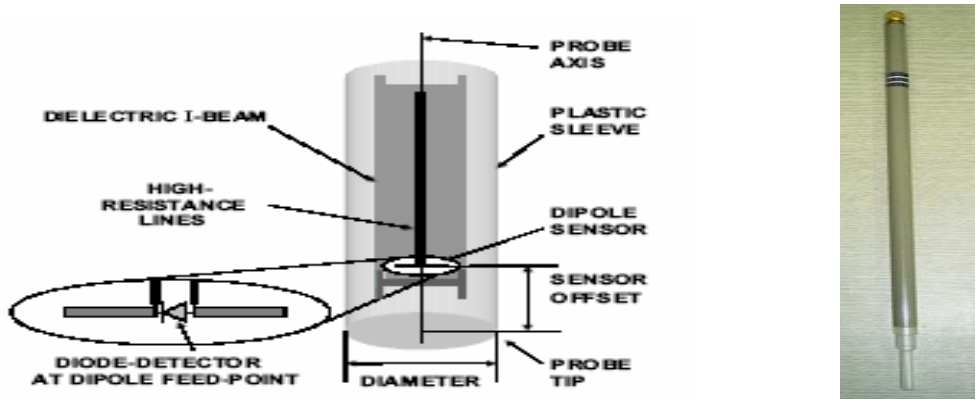

Figure 1. E-field probe features near probe tip end (left) [2] and picture of the complete probe with the plastic rod containing RF transparent transmission line (right) [3].

2. Boundary Proximity Effects of an E-field Probe

Boundary proximity effects arise when the tip of an E-field probe approaches the interface between two dielectric media in Fig 2. Under these conditions, the external field is strongly perturbed by the superposition of a scattered field from the dielectric probe surface and from the dielectric phantom surface.

ISBN: 89-86522-78-0 94460©KEES

The error due to boundary proximity effects is known to be typically less than 2% if the distance between the probe tip and the surface is greater than half the probe diameter [2].

In general, the local peak SAR values occur at the surface of the phantom and are not directly measurable by the field sensors which are usually located 2–3 mm along the axis behind the probe tip, which was named 'sensor offset' in Fig 1 (left). The SAR values between the nearest measured point and the surface are determined by extrapolation methods in Fig 2 (left). In practice, there is a tradeoff between increased distance to reduce the boundary proximity effects and the resulting possible increase in extrapolation error.

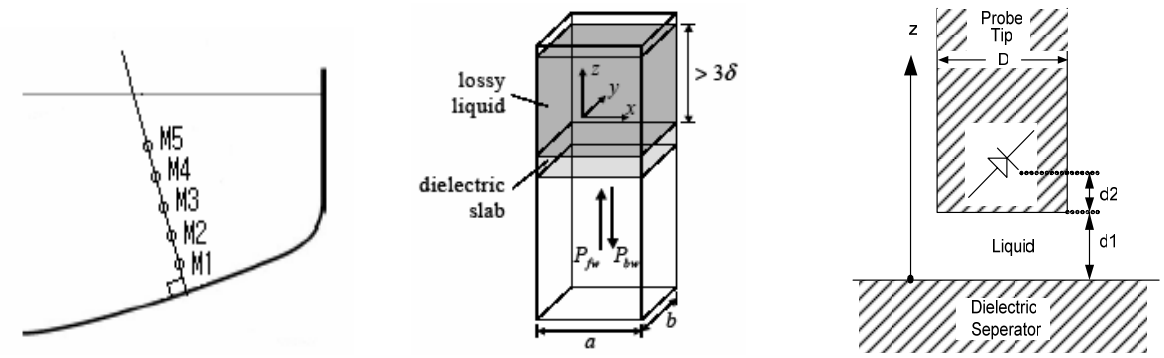

Figure 2. Orientation of the probe corresponding to the line normal to the surface. M1–M5 are example measurement points used for extrapolation to the surface [2](left). / Vertical rectangular waveguide calibration setup [4](middle). / ab= 0.2476 m x 0.1238 m for 835 MHz. / Probe tip geometry in the lossy waveguide in detail (right). sensor offset d2 = 2.25 mm, scanning along z-axis: 0 ≤ d1 ≤ 50 mm, tip diameter D=4.8 mm.

3. Calibration and characterization of dosimetric probes

Probe calibration is usually done with two-step methods, where the total field is given by Equation (2):

$$|E|^2 = \sum_{i=1}^{3} |E_i|^2 = \sum_{i=1}^{3} \frac{f_i(V_i)}{\eta_i \psi_i} \qquad (2)$$

Here, E_i (i = 1, 2, 3) are the components resulting from the projection of the E-field vector on the three orthogonal sensors, f_i (V_i) is a linearizing function of the rectified sensor signal V_i in the form of $V_i + V_i^2/DCP_i$ [5] in [mV], η_i in [μV/(V/m)^2] is the sensitivity of sensor dipole i in air for the sensor aligned with the field vector, and ψ_i is the ratio of sensor response in air to response in the dielectric media and sometimes referred to as the conversion factor.

In the setup in Figure 2 (middle), a portion of an upright-standing open waveguide is filled with a tissue-equivalent liquid, and TE_{10} mode in the liquid can be analyzed by some equations.

$$H_x = (j\beta a/\pi) A_{10} \sin(\pi x/a) e^{-\alpha z} e^{-j\beta z},\ E_y = (-j\omega\mu a/\pi) A_{10} \sin(\pi x/a) e^{-\alpha z} e^{-j\beta z} \qquad (3)$$

$$k^2 = \omega^2 \mu_0 \varepsilon_0 (\varepsilon_r' - j\varepsilon_r'') = (\pi/a)^2 + (\beta - j\alpha)^2 = (\pi/a)^2 + (\beta^2 - \alpha^2) - j2\alpha\beta \qquad (4)$$

$$\beta = \sqrt{\alpha^2 + \omega^2 \mu_0 \varepsilon_0 \varepsilon_r' - (\pi/a)^2},\ \omega^2 \mu_0 \varepsilon_0 \varepsilon_r'' = 2\alpha\beta,\ \omega\varepsilon_0\varepsilon_r'' = \sigma = 2\alpha\beta/(\omega\mu_0) \qquad (5)$$

The penetration depth δ, which is the reciprocal of α, is determined from equation (4) and (5),

$$\delta = \alpha^{-1} = \left\{ \mathrm{Re}\left[\sqrt{(\pi / a)^2 + j\omega\mu_0(\sigma + j\omega\varepsilon_0\varepsilon_r')} \right] \right\}^{-1} \quad (6)$$

The power flow at the input port of the waveguide is,

$$P_{in} = \frac{1}{2}\mathrm{Re}\int_{x=0}^{a}\int_{y=0}^{b} \overline{E} \times \overline{H}^{*} \cdot \hat{z}\,dy\,dx = \frac{\omega\mu a^3 b\beta}{4\pi^2}\left|A_{10}\right|^2 e^{-2\alpha z}\Big|_{z=0} = \frac{\omega\mu a^3 b\beta}{4\pi^2}\left|A_{10}\right|^2 \quad (7)$$

To calculate SAR inside of waveguide with the lossy liquid,

$$\left|E_y\right|^2 = E_y E_y^{*} = \frac{\omega^2\mu^2 a^2}{\pi^2}\left|A_{10}\right|^2 \sin^2\frac{\pi x}{a} e^{-2\alpha z} = \frac{4P_{in}\omega\mu}{ab\beta}\sin^2\frac{\pi x}{a} e^{-2\alpha z} \quad (8)$$

$$SAR(z) = \frac{\sigma\left|E\right|^2_{phasor}}{2\rho} = \frac{\alpha}{\rho}\frac{4P_{in}}{ab}\sin^2\frac{\pi x}{a} e^{-2\alpha z} = \frac{4(P_{fw} - P_{bw})}{\rho ab\delta}\sin^2\frac{\pi x}{a} e^{-2\alpha z} \quad (9)$$

4. Extrapolation of E-field Near the Dielectric Boundary

The boundary proximity effect of the probe was checked by driving 835 MHz, 1.0 W input power to the waveguide in Fig 2.(middle), with measured dielectric constant of the tissue 40.8, measured conductivity of the tissue 0.90 [S/m], and conversion factor Ψi = 4.988. More geometry in detail of the probe in waveguide is shown in Fig 2(right). $\Sigma f_i[V_i(z)]/\eta_i$ in equation (2) and SAR values on equation (1) were measured along the z-axis and extrapolated in Table 1 near the boundary surface.

Table 1. Measured or extrapolated values related with the SAR (z) along the z-axis at the central point of the dipole sensor of the probe where the detection diodes are located.

z - axis (d1+ d2,mm)	$\sum \frac{f_i(z)}{\eta_i}$ $k(V/m)^2$ (Measured)	$\sum \frac{f_i(z)}{\eta_i} \Big/ \sum \frac{f_i(z+1)}{\eta_i}$ (Measured)	$\sum \frac{f_i(z)}{\eta_i} \Big/ \sum \frac{f_i(z+1)}{\eta_i}$ (Extrapolated)	$\sum \frac{f_i(z)}{\eta_i}$ $k(V/m)^2$ (Extrapolated)	Point SAR [W/kg] (Measured) (** Extrapolated)
0	Not available	Not available	1.05591	18.16178	3.277**
1	Not available	Not available	1.05591	17.20017	3.104**
2	Not available	Not available	1.05591	16.28947	2.939**
2.25	18.80230	1.18099* (presumed)			3.393
3	16.29313	1.09687	1.05591	15.42699	(2.784**) 2.940
3.25	15.92072 (presumed)				
4	14.85410	1.07353	1.05591	14.61018	(2.636**) 2.680
5	13.83661	1.06424			2.497

* Value ratio measured at z = 2.25 mm to the presumed value at z = 3.25 mm.

Detected probe voltage ratio at z [min] and at z+1 [min] in Table 1 are shown in Fig 3 (left).

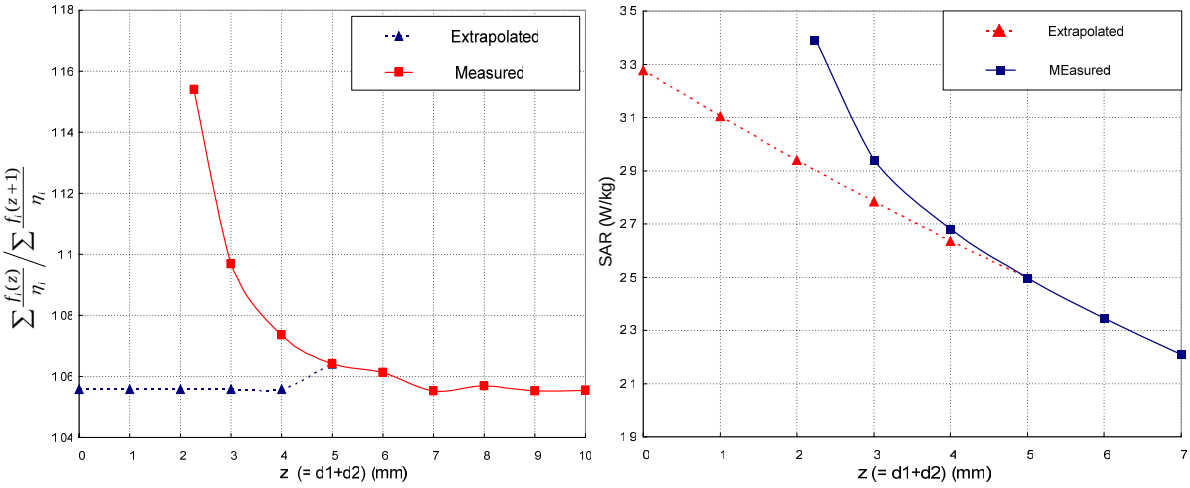

Figure 3. Ratio of the measured or extrapolated $|\overline{E}|^2$ near the dielectric separator surface to the $|\overline{E}|^2$ value at 1 mm farther away to the waveguide end direction along the guide axis in Fig. 2 / (left), and correlated point SAR from 6th column of Table 1 (right).

We can see in Fig 3 (left) that boundary proximity effect begins from z=d1+d2=7 mm up to the sensor offset distance. But the effect is minor until z=5 min, so the extrapolations are performed z=5 mm to 0 mm.

The triangular points shown in Figure 3 represent the SAR values extrapolated at 1 mm steps for the points next to the phantom surface that cannot be measured.

The difference of extrapolated SAR value starting from 5 mm and from 7 mm is less than 3 % (2.9 %) in this measurement. For a very small boundary proximity error, maybe less than 1 %, the extrapolation distance from boundary surface to the probe tip end should be the length of the probe tip diameter.

[References]

[1] ICNIRP Guidelines, Guidelines for Limiting Exposure to Time-varying Electric, Magnetic, and Electromagnetic Field (up to 300 GHz), international Commission on Non-ionizing Radiation protection, 1998.

[2] IEEE Std 1528™-2003, IEEE Recommended Practice for Determining the Peak Spatial-Average Specific Absorption Rate (SAR) in the Human Head from Wireless Communication Devices: Measurement Techniques, IEEE Standards Coordinating Committee 34, 2003.

[3] Catalog of SAR Measurement System ESSAY III, EMF Safety Inc, 2004.

[4] Pokovic, K., "Advanced Electromagnetic Probes for Near-Field Evaluation," Doc. Tech. Sci. Diss. ETH Nr. 13334, Swiss Federal Institute of Technology, Zurich, Switzerland, 1999.

[5] Young-Myoung Gimm, Seoung-Bae Lee, Kee-Hoe Kim "Linearity Characteristics of the Detection Voltage of an E-Field Sensing Probe in SAR Measurement System," 2004 Korea-Japan Joint Conference on AP/EMC/EMT, Seoul, Korea, pp. 321-326, June 2004.